Photorefractive measurements in electron irradiated semi-insulating GaAs

Philippe Delaye, H.J. von Bardeleben, Gérald Roosen

Photorefractive measurements in electron irradiated semi-insulating GaAs

P. Delaye[(1)], H.J. von Bardeleben[(2)], G. Roosen[(1)]

[(1)] Institut d'Optique Théorique et Appliquée, Unité de Recherche Associée 14 au Centre National de la Recherche Scientifique, Bât.503 - Centre Scientifique d'Orsay, B.P. 147 - 91403 ORSAY Cedex

[(2)] Groupe de Physique du Solide, Unité de Recherche Associée 17 au CNRS, Université Paris 6 et Paris 7 - 2, Place de Jussieu - 75005 PARIS

ABSTRACT :

We present photorefractive measurements at 1.06μm and 1.3μm performed in electron irradiated GaAs. Irradiation with electrons of kinetic energies ≥ 1MeV introduces intrinsic electrically active defects, which modify the Fermi level position and allow to modify the electron hole competition mechanism of the photorefractive effect. Further, it has been shown that the optical absorption in the 1.3 to 1.5 μm spectral range can be increased, which might allow to enlarge the useful spectral range of GaAs towards optical telecommunication windows. The native and irradiation induced defects have been assessed by electron paramagnetic resonance and optical absorption spectroscopy conducted at T=300K and 77K. The direct influence of an irradiation induced mid-gap defect on the photorefractive effect is experimentally and theoretically demonstrated .

PACS : 71.55.Eq, 78.50.Ge, 42.70.Nq

I. INTRODUCTION

The photorefractive (PR) effect in electrooptic photoconductive semiconductor materials is related to the optically induced charge redistribution between deep defect levels. In the semi-insulating III-V materials GaAs and InP, one deep defect is responsible for both photocreation and trapping of free carriers : it is the EL2 and the Fe_{In} defects, respectively. Both defects introduce a deep level ($EL2^{0/+}$ and $Fe^{-/0}$), situated around mid-gap, which pins the Fermi level. Different studies have been performed in order to analyze the influence of these defects on the PR effect in these materials [1-5].

In undoped, liquid encapsulated Czochralski grown GaAs, the EL2 defect is present at concentrations [EL2] ≈ (2 ± 1) x 10^{16} cm^{-3}. The occupancy of the EL2 defect is very variable from one sample to another depending on the growth characteristics and on the concentration of the residual contaminants in the sample. The occupancy ratio $[EL2^{+}]/[EL2^{0}]$ does vary from 0.1 to 1 depending on the growth conditions. Modern state of the art material is characterized by an occupation ratio < 0.1, which is not optimal for PR applications. The photorefractive properties of GaAs are very dependent on this ratio, especially around 1.3μm [3], because of the electron-hole competition. The occupancy ratio, one would like to have for wavelengths around 1.3μm, is greater than 1. We propose in this paper a new approach, based on the irradiation with high energy electrons, to control the occupation ratio, which is expected to improve the PR response at 1.3 μm. Irradiation creates in the gap a variety of deep defects that change the compensation mechanism in the material, inducing a change in the Fermi level position. We will show in the following, that the irradiation indeed leads to an increase of the $[EL2^{+}]/[EL2^{0}]$ ratio.

The outline of the paper is the following. After a presentation of electron irradiation induced defects in GaAs, we present results of electron paramagnetic resonance (EPR) and optical absorption measurements, which are performed in order to monitor the change in the occupation ratio of EL2 and the introduction of the irradiation induced defects. We then present the PR effect measurements realized in the electron irradiated samples. We show that our results can be interpreted in a two defect PR model, which includes, besides the EL2

defect, only one of the irradiation induced defects, H3, which introduces a mid-gap level equally.

II. ELECTRONIC IRRADIATION

A. sample and irradiation characteristics

To analyze the effect of irradiation in undoped semi-insulating GaAs, we use a set of samples issued from the same ingot. These samples are characterized before irradiation by a total EL2 concentration [EL2]=1.3x10^{16} cm^{-3} and a compensation ratio [$EL2^{+}$]/[$EL2^{0}$] close to 1 [3].

The samples are irradiated with electrons of kinetic energy higher than the displacement threshold of atoms (200keV). We choose an energy of 2MeV, which allows to have defect introduction rates in the order of $10^{-2}cm^{-1}$ and gives rise to a homogenous defect distribution over the thickness of the sample (≈1.5mm) The irradiation doses are chosen between 1 and 5 x 10^{16} electrons per squared centimeters. The irradiation is performed at room temperature.

B. irradiation induced defects

The defects created by electron irradiation in n and p-type samples and particularly their electrical properties have been studied before [6]. The primary defects created by irradiation are Frenkel pairs (V_{As}—As_i, V_{Ga}—Ga_i) in the two arsenic and gallium sublattices. Recently it has been demonstrated [7, 8] that the formation of antisite defects, As_{Ga} and Ga_{As} also takes place with high introduction rates. All these intrinsic defects are electrically active and their presence will modify the Fermi level and also the lifetime of the free carriers.

The electrical properties of the defects introduced in n- and p-type GaAs have been determined by Deep Level Transient Spectroscopy (DLTS) [6]. These defects have been

classified as electron traps called E1 to E5, and holes traps called H0-H3. All these defects are stable at room temperature and may play a role in our experiments.

Table 1 gives some of the parameters of these defects [6]. T_0 is the temperature of the DLTS peak (corresponding to a thermal emission coefficient of $70s^{-1}$). τ is the introduction rate of the defect and, if Φ is the flux of electrons (in cm^{-2}), the concentration of created defects is $N_T = \tau\Phi$. E_e is the energy level of the defect, taken from the conduction band for electron traps E and from the valence band for hole traps H. σ_a is the apparent capture cross-section (σ_{na} for the capture of electrons of the conduction band by traps E and σ_{pa} for the capture of holes of the valence band by traps H). Thermal emission coefficient ß as a function of temperature T is given by [9, 10] :

$$\beta_n = 2.28 \times 10^{20} \; T^2 \; \sigma_{na} \; exp\left(\frac{-E_e}{k_B T}\right)$$

$$\beta_p = 1.7 \times 10^{21} \; T^2 \; \sigma_{pa} \; exp\left(\frac{-E_e}{k_B T}\right)$$

with E_e and σ_a given in Table 1. We then calculate the value of ß at T=300K ($ß_n$ for electron traps and $ß_p$ for hole traps).

The electron and hole traps E and H have been evidenced both as majority and minority carrier traps. Thus they are expected to be present in all samples independently of their conductivity type and in particular in semi-insulating samples, for which no quantitative electrical measurements are possible. All the characteristics of the defects of Table 1, can be used for our semi-insulating samples. The only parameter, which is expected to vary with the conductivity of the sample, is the introduction rate τ given in Table 1 for n- and p- type samples. A RPE measurement has given an introduction rate of arsenic antisite varying from $1cm^{-1}$ in n-type samples to $10^{-2}cm^{-1}$ in semi-insulating samples.

Table 1 gives us some important informations on the defects created by irradiation and on their eventual influence on the PR effect. The introduction rate of the different defects, in our semi-insulating crystals, is expected to be of the order 10^{-2} to $1cm^{-1}$,which means that defects are introduced in concentrations of typically $10^{15}cm^{-3}$ for the electron dose ($10^{16}e^{-}.cm^2$) we have chosen. The next point concerns the thermal emission rate of defects. Studies of the PR effect have shown that the optical emission rate of carriers must exceed

their thermal emission rate [11]. A high thermal emission coefficient will be thus prejudicial to the PR properties of a given defect. The occupancy ratio of the defect is another important parameter for the PR effect (it will appear later in the effective trap density N_{eff}). We now discuss this point at the light of the results given in Table 1. The occupancy ratio depends on the position E_a of the energy level of the defect compared to E_f the Fermi level position. For example, for an acceptor level A which can exist under two states of charge : neutral A^0 (concentration N_a^0) and with a valence band electron captured A^- (concentration N_a^-), we have a ratio of concentrations :

$$\frac{N_a^0}{N_a^-} = g_a \, exp\left(\frac{E_a - E_f}{k_B T}\right)$$

with g_a a degeneracy factor which value is in general close to 1. As soon as $|E_a - E_f|$ is greater than $4k_BT$ (k_BT=0.025eV at T=300K), $\frac{N_a^0}{N_a^-}$ becomes smaller than 10^{-2} (i.e. a small value of the effective trap density $N_{eff} = \frac{N_a^- \; N_a^0}{N_a^- + N_a^0}$). A similar argument can be used for a donor level, leading to the same conclusion.

In our semi-insulating sample, the Fermi level is pinned before irradiation on the 0/+ level of the native EL2 defect, i.e. $E_f \approx 0.7$eV (from the conduction band). After irradiation the samples stay semi-insulating, and the Fermi level changes only a little (as it will be shown by our EPR and optical absorption results), which means that the Fermi level stays around 0.7eV. We see in Table 1 that all the irradiation defects, except H3 and E4, are at least 0.2eV away from the Fermi level. So they are all in one charge state only (empty of electrons for E traps and full of electrons for H traps). All these defects are thus characterized by a very small effective trap density, which means that they will have a negligible influence on the PR effect.

For this reason we will consider only the two defects H3 and E4 for the analysis of the PR results in the following. The generation and recombination of holes is expected to be determined by the H3 defect .

III. SAMPLE CHARACTERIZATION

Before measuring and analyzing the photorefractive properties of the electron irradiated samples we present in this section the results, obtained by Electron Paramagnetic Resonance (EPR), absorption and electrical conductivity measurements on the same samples.

A. Electron paramagnetic resonance

EPR measurements have been performed on the as-grown and on the electron irradiated samples in order to determine the variation of the Fermi level position via the change in the occupation ratio of the EL2(0/+) level and the introduction of electron irradiation induced paramagnetic defects. It has been shown before, that the electron irradiation does not modify the total EL2 concentration itself [12]. The EPR measurements have been performed with an X-band spectrometer ; the measuring temperature was between 4K and 16K. The utilization of a spin standard sample (Al_2O_3:Cr) allows to determine quantitatively the defect ($EL2^+$) concentration. The defects were measured under thermal equilibrium conditions and under 1.05μm optical excitation, the wavelength leading to the quenching of the EL2 related As_{Ga} spectrum..

Previous EPR studies have allowed the assignment of microscopic models for three irradiation induced defects [13]: an Arsenic antisite defect with slightly modified EPR parameters as compared to the EL2 defect and no optically induced metastability, the Gallium antisite defect and the Gallium vacancy defect.

Before irradiation the samples show only one paramagnetic defect, whose Spin Hamiltonian parameters identify it as the positively charged EL2 defect (Fig.1) (g-factor g=2.03 and hyperfine interaction constant $A=890\times10^{-4}cm^{-1}$ [14]). The concentration of this defect is determined to be $6.6\times10^{15}cm^{-3}$. This defect is completely quenchable.

After a first irradiation with a dose of $1\times10^{16}e^-.cm^{-2}$ the concentration of the positively charged As_{Ga} defect is increased by ≈30% to a value of 9.2×10^{15} spin.cm^{-3}. Further

irradiation up to a final dose of $5x10^{16}cm^{-2}$ does no longer modify this concentration (Table 2). The fact that the As_{Ga}^{+} concentration is not further modified does not imply, that no further defects are created by the irradiation ; it only demonstrates, that the compensation ratio N_D-N_A stays constant. In addition to the native As_{Ga} defect (related to EL2) we observe equally the irradiation induced As_{Ga} defect, the EPR spectrum of which is not quenchable (Table 2). The values of Table 2 show that the irradiation changes the $EL2^{+}$ concentration changes by ≈10% only.

In addition to the EL2 related arsenic antisite defect we observe under optical excitation a different EPR spectrum, which we have assigned previously to the Ga_{As}^{-} defect (Fig.1). The intensity of this spectrum increases linearly with the irradiation dose (Table 2). The optical properties of this defect and in particular the photoionization spectra of the 2-/- charge states have not been measured yet. It seems however, that the Ga_{As} 2-/- level can be associated with the H1 level at E_V+0.25eV. Consequently low temperature photoexcitation at 1.2eV is expected to photoionize the Ga_{As}^{2-} defect transferring a free electron in the conduction band.

B. Absorption

The absorption spectra for all our samples are deduced from measured transmission spectra at room temperature using an expression that take into account multiple reflections : $T = \frac{(1-R)^2 exp(-\alpha l)}{1-R^2 exp(-2\alpha l)}$. Coefficient of reflection R is calculated with the value of the refractive index given by Ref.[15, 16]. Results are given in Table 3 for the two wavelengths of interest 1.06μm and 1.32μm. Following the irradiation dose we observe an increase of absorption for the two wavelengths, which is seen over the whole spectrum (Fig.2), with a smooth bump around 1.3μm. From the absorption spectra of the non irradiated sample (D2) at room temperature (Fig.2), we deduce the total concentration of the EL2 defect. We use the wavelength of 1.19μm [17] where electron and hole photoionization cross-sections are equals : S_n=S_p=$4.9x10^{-17}cm^2$ [18]. At λ=1.19μm, we have α=$0.65cm^{-1}$ which gives for the EL2 total concentration, [EL2]=$1.3x10^{16}cm^{-3}$. This parameter is important as the electronic

irradiation does not affect the total concentration of EL2 but only the occupancy ratio of the defect ($[EL2^+]/[EL2^0]$). So we take this value of concentration, determined in the non irradiated sample, for all the other irradiated samples.

Complementary absorption measurements are performed at low temperature (T=77K). They will provide much more information. Several reasons call for these measurements. Firstly absorption band widths depend on temperature and smaller temperatures will lead to thinner bands and then, more distinct features in the absorption spectra. The second and main reason is that, at this temperature, we can use the quenching properties of EL2 defect [19]. The disappearance of the absorption bands related to the EL2 defect will reveal other absorption bands related to irradiation induced defects. This quenching phenomenon is illustrated in Fig.3 where we see the absorption spectra of sample D2 (non irradiated) before and after quenching of EL2 defect by illumination of the sample with the light of a Nd:YAG laser emitting at 1.06μm. The nearly total disappearance of absorption confirms that EL2 is the main defect for the absorption of the samples before irradiation. The slightly negative absorption observed in Figure 3 at long wavelength is certainly due to an overestimation of about 2% of the index of refraction (and thus of R), which value was given at 103K in ref.[16] and not at 77K, temperature where our experiment is performed.

In irradiated samples after quenching of EL2 absorption, we see the appearance of an absorption band centered at 1.32μm, as well as an absorption tail near the gap (Fig.4) which both increase with the irradiation dose. The absorption tail is caused by the multiple defects that are created close to valence and conduction band. At the wavelengths of interest (1.06μm and 1.32μm) this absorption tail has only little influence, so we do not discuss it further. The absorption band centered at 1.3μm covers the range of interest and grows linearly with the irradiation dose (Fig.5). We attribute this absorption band to the photoemission of holes from the H3 defect, the photoionization cross-section spectrum of which has been determined by Deep Level Optical Spectroscopy experiments in p-type crystals [20]. This spectrum, presented in Figure 6, corresponds exactly to the absorption spectra we measure (Fig.4). The electron photoionization cross-section spectra for E4 defect is not known. We assume it to be similar to the electron photoionization cross section spectra of $EL2^0$ [21] (i.e. a strong

influence of the higher L and X conduction bands). This means that E4 is partly responsible for the absorption tail near the gap and is of low influence at 1.06μm and at 1.32μm compared to the absorption due to H3. Thus H3 only has to be considered in the spectral region we use.

C. Conductivity

We perform dark conductivity and photoconductivity measurements in the different irradiated and non irradiated samples. The ohmic contacts are realized with silver paint. The characteristics is ohmic at low applied field (smaller than 300V.cm^{-1}) in all the samples.

We observe an increase of the dark conductivity of the samples with the irradiation dose (Table 4). When high fields are applied, we observe a non-ohmic behavior in the sample, which corresponds to the field enhancement of the capture cross-section of electrons on the EL2 defect [22]. Note that this non-ohmic character decreases with increasing dose of irradiation corresponding to a decreasing role of the EL2 defect on the dark conductivity.

Photoconductivity measurements are performed at the two wavelengths of 1.06μm and 1.32μm with an incident illumination on the crystal of 16mW.cm^{-2} for both wavelengths. We observe a decrease of the photoconductivity with the dose of irradiation (Table 4). The photocurrent is verified to be linear with the illumination.

This decrease of photoconductivity and increase of dark conductivity cannot be explained by the observed variations of the EL2 occupancy ratio. Another reason is that the modification of this ratio goes through an increase of the role of holes as EL2^{+} increases, that would lead to an increase of photoconductivity at 1.32μm as this photoconductivity is mainly due to holes. Thus, the natural way to explain the observed feature of the conductivity is to introduce a second defect, which can be the H3 and/or E4 defect. For dark conductivity, as electrons are predominant, the effect of the secondary defect is mainly to increase the number of free carriers and then to increase conductivity. For photoconductivity the effect is different, as mainly holes are generated at 1.06μm and 1.32μm as well. Valence band is emptied from these holes by recombination on the H3 defect, when it is created by irradiation, and

photoconductivity decreases. In fact the effects are much more complicated than here presented and only numerical simulations can show the precise effect of irradiation on conductivity. Unfortunately, even in a simplified model where we neglect the charge redistribution in the levels (i.e. Fermi level variation) induced by irradiation, the number of unknown parameters is too important for the simulation to be reliable. The important point stays that it is necessary to introduce this secondary defect to explain the photoconductivity results.

D. Conclusion on sample characterization

The results of our combined EPR, absorption, and conductivity measurements lead to the conclusion that electron irradiation shifts the Fermi level position such as to obtain an occupancy ratio for EL2 close to one and creates one mid-gap defect H3, a hole trap, responsible for the absorption band centered at 1.3μm. This defect influences both the dark and photoconductivity of the irradiated samples. Its presence will also be sensitive in PR measurements and will require an extension of the PR model to a two defect model comprising EL2 and H3 as it will be seen in the following.

IV. PHOTOREFRACTIVE EFFECT IN IRRADIATED GaAs

The photorefractive effect in undoped semi-insulating GaAs is based on optical and electrical properties of the native defect EL2. At 1.32μm the performances of such a sample are strongly dependent on the occupancy ratio of this defect [3]. The irradiation will change the position of the Fermi level, which will become closer to the valence band. It will lead to an increase of the role of the holes in the PR effect and then an improvement of this mechanism in these materials at 1.32μm [23].

A. Set-up and experimental results

We study the photorefractive effect by a two-beam coupling experiment. We measure the energy transfer gain $\gamma_0 = \frac{I_s(with\ \ Pump\ \ beam)}{I_s(without\ \ Pump\ \ beam)}$ from a strong pump beam toward a weak probe beam I_s from which we deduce photorefractive gain Γ with expression $\gamma_0 = e^{-\Gamma d}$ (d thickness of the sample). The measurement is performed with two diode pumped Nd:YAG lasers emitting at 1.06μm and 1.32μm. These lasers emit vertically polarized beams that are splitted and then recombined on the crystal in order to form an interference pattern with a grating spacing Λ (or grating wave number k=2π/Λ). The grating vector is oriented along the [001] crystal axis and beams are polarized along the [110] crystal direction.

The theoretical variation of photorefractive gain Γ with k is given by an expression developed with the model taking into account bipolar conduction [24, 25] (hole-electron competition) in the case of grating spacings smaller than the diffusion length of the carriers :

$$\Gamma = \frac{2\pi\ \ n_o^3\ \ r_{41}}{\lambda\ \ cos\theta}\frac{k_B T}{e}\ \ \frac{\xi_0 k}{1+k^2/k_o^2}$$

with : $\xi_0 = \frac{S_n\left[EL2^o\right] - S_p\left[EL2^+\right]}{S_n\left[EL2^o\right] + S_p\left[EL2^+\right]}$ and $k_o^2 = \frac{e^2}{\varepsilon\ \ k_B T}\frac{\left[EL2^o\right]\left[EL2^+\right]}{\left[EL2^o\right]+\left[EL2^+\right]}$

In these expressions n_0 is the refractive index of the material (n_0 = 3.44 at 1.06μm, and n_0 = 3.38 at 1.32μm [15, 16]); r_{41} is the electrooptic coefficient (r_{41} =1.72pm.V^{-1} at 1.06μm and r_{41} =1.54pm.V^{-1} at 1.32μm [26]), θ is the half-angle between the beams inside the crystal (we have for all grating spacings cosθ ≈1), ε is the static dielectric constant (ε=1.13x10^{-10} F.m^{-1} [16]).

ξ_0 is the hole-electron competition coefficient and k_o^2 is the inverse squared of the Debye screening length. These parameters depend on the photoionization cross-sections of carriers (S_n for electrons and S_p for holes) from the deep level EL2 (wavelength dependent parameter) [18] and on the concentrations of the two states of charge of the EL2 defect (wavelength independent parameter).

Experimental results are presented in Table 5. For each sample and each wavelength we verify that the gain saturates with respect to the incident irradiation. We also eliminate the absorption grating components which are present in highly irradiated samples by using properties of symmetry of the PR effect [27]. Γ changes its sign when turning round the crystal of 180° around the [110] direction, whereas absorption components stay identical which allows the extraction of the photorefractive component for all the measurements as presented in Table 5.

We experimentally observe a decrease of the gain at 1.06μm with the irradiation dose leading to a complete cancellation of the gain for the highest dose. Nearly no change is observed at 1.32μm.

For the non irradiated sample D2, we estimate from the measurements at 1.06μm an hole-electron competition coefficient $\xi_0 \approx 0.7$, which gives, taking into account the absorption of this sample $\alpha = 1 cm^{-1}$, $\alpha_n = S_n [EL2^0] \approx 0.8 cm^{-1}$ and $\alpha_p = S_p [EL2^+] \approx 0.2 cm^{-1}$. We know from our absorption and EPR measurements that $[EL2^+] = 6 \times 10^{15} cm^{-3}$ and $[EL2^0] = 7 \times 10^{15} cm^{-3}$. With the photoionization cross-sections taken in the literature [18] : $S_n = 10^{-16} cm^2$ and $S_p = 4 \times 10^{-17} cm^2$, we can then calculate $\alpha_n = 0.7 cm^{-1}$ and $\alpha_p = 0.25 cm^{-1}$, which corresponds to the experimental estimation using PR measurements. After irradiation with a dose of 5×10^{16} $e^-.cm^{-2}$ (sample D8) we have $\xi_0 \approx 0$, which would lead to $\alpha_n \approx \alpha_p$. For this sample we have $[EL2^+] = 7 \times 10^{15} cm^{-3}$ (given by EPR measurements (Table 2)) and then $[EL2^0] = 6 \times 10^{15} cm^{-3}$, from which we calculate $\alpha_n = 0.6 cm^{-1}$ and $\alpha_p = 0.3 cm^{-1}$ and $\xi_0 \approx 0.3$, values very different from what is observed experimentally.

If we would consider that the change of the photorefractive gain at 1.06μm was due to a change of the $[EL2^+]/[EL2^0]$ ratio, we should have observed an increase of a factor 2 to 3 of the gain at 1.32μm, which, obviously, does not exist. Moreover, as seen in EPR experiments, the ratio changes a little only with the irradiation dose and not enough to explain the change of photorefractive gain at 1.06μm.

So, the one defect hole-electron competition model which explains the PR effect in non irradiated GaAs in the 1-1.5μm range [3] and sample D2, fails to explain the photorefractive response of electron irradiated GaAs. We have to take into account the secondary defect

created by irradiation that we saw in absorption experiments. We will now describe this model and then show how it applies to the case of electron irradiated GaAs.

B. Photorefractive effect modeling with a secondary trap and hole-electron competition

Recently an extension of the photorefractive model which takes into account a main defect coupled with both conduction and valence band and a secondary defect coupled with either the conduction band or the valence band (Fig.7) was developed [28]. The analytical expression of the photorefractive gain with a secondary hole trap (coupled with the valence band) is :

$$\Gamma = \frac{2\pi}{\lambda}\frac{n_o^3 r_{41}}{\cos\theta}\frac{k_B T}{e}\frac{k}{1+\frac{k^2}{k_o^2+k_o'^2}}\left[\frac{k_o^2\xi(k)}{k_o^2+k_o'^2}-\frac{k_o'^2}{k_o'^2+k_o^2}\left[\frac{1}{A_p'}-\frac{\xi(k)-\frac{1}{A_p}}{1+\frac{k^2}{\kappa_p^2}}\right]\right]$$

with $\xi(k)=\dfrac{\left(\alpha_n-\alpha_p\right)k^2+\left(\alpha_n\kappa_p^2-\alpha_p\kappa_n^2\right)}{\left(A_n\alpha_n+A_p\alpha_p\right)k^2+\left(A_n\alpha_n\kappa_p^2+A_p\alpha_p\kappa_n^2\right)}$

$k_0^2=\dfrac{e^2}{\varepsilon\ k_B T}\ \dfrac{N_0\left(N_T-N_0\right)}{N_T}$ and $k_0'^2=\dfrac{e^2}{\varepsilon\ k_B T}\ \dfrac{N_0'\left(N_T'-N_0'\right)}{N_T'}$ are linked to the Debye screening length of the two defects and we have $\alpha_n=S_n\left(N_T-N_0\right)$, $\alpha_p=S_pN_0$, $A_n=\dfrac{\beta_n+S_nI_0}{S_nI_0}$, $A_p=\dfrac{\beta_p+S_pI_0}{S_pI_0}$, $A_p'=\dfrac{\beta_p'+S_p'I_0}{S_p'I_0}$, $\kappa_p^2=\dfrac{e}{k_BT}\ \dfrac{\gamma_p\left(N_T-N_0\right)}{\mu_p}$, $\kappa_n^2=\dfrac{e}{k_BT}\ \dfrac{\gamma_nN_0}{\mu_n}$.

In these expressions S represents the photoionization cross-section, ß the thermal emission coefficient, γ the recombination coefficient and μ the mobility. N_T-N_0 is the concentration of neutral traps and N_0 the concentration of ionized traps. The prime corresponds to the secondary defect, n and p indices deal with electrons and holes respectively.

We see on this expression that the influence of the secondary defect occurs through the two terms $k_0'^2$ and A_p' only. We can then understand in what conditions a secondary defect effectively influence the PR effect. The first point deals with term A_p' which is linked to the thermal emission coefficient $ß'_n$ of the secondary defect. For example, for most of the defects of Table 1 this coefficient is greater than S_nI_0 (which is of the order of magnitude of $10s^{-1}$ for

typical illumination I_0 of some hundreds of mW.cm^{-2} and value of S_n around 10^{-16} cm^2), which means that in most of the cases we have $\frac{1}{A'_p} << 1$. The second point to discuss is the value of k'^2_0 or the value of the effective trap density $N'_{eff} = \frac{N'_0\left(N'_T - N'_0\right)}{N'_T}$ of the secondary defect. The effective trap density of the main defect is generally greater than 10^{15}cm^{-3}, value we will use as a reference. We saw previously that a defect located at more than $4k_BT$ from the Fermi level is characterized by a ratio $\frac{N'_0}{\left(N'_T - N'_0\right)} < 10^{-2}$ (or $\frac{\left(N'_T - N'_0\right)}{N'_0} < 10^{-2}$ according to the position above or below the Fermi level) and then an effective trap density $N'_{eff} < 10^{-2} N'_T$ for defects introduced with concentrations $N'_T < 10^{16} cm^{-3}$. All the defects of Table 1 are at more than 0.2eV from the Fermi level except H4 and E3, so these defects will be characterized by very low effective trap densities and we will have for all these defects $k'^2_0 << k_0^2$. In conclusion, in semiconductors around room temperature and with moderate illumination (some hundreds of mW.cm^{-2}) it will be necessary to take into account a secondary defect only if it is sufficiently close to the Fermi level to be under two states of charge and have a moderate thermal emission coefficient or if it is present in high concentration in order to compensate for its distance from the Fermi level.

C. Discussion of results

In the case of semiconductors the previous expression of the gain can be simplified by doing the usual approximation of grating spacing smaller than the diffusion length (i.e. $k^2 >> \kappa_n^2, \kappa_p^2$). In that case we have $\frac{1}{1 + \frac{k^2}{\kappa_p^2}} << 1$ and $\xi(k)$ becomes $\xi(k) = \frac{\left(\alpha_n - \alpha_p\right)}{\left(A_n\alpha_n + A_p\alpha_p\right)}$.

We also suppose that the illumination is sufficient to assure that the gain does not vary with illumination, i.e. that $A_n = A_p = A'_p = 1$. We then have an expression of the photorefractive gain that reduces to :

$$\Gamma = \frac{2\pi}{\lambda} \frac{n_o^3 r_{41}}{\cos\theta} \frac{k_B T}{e} \frac{k}{1 + \frac{k^2}{k_o^2 + k'^2_o}} \left[\frac{k_o^2 \xi_0 - k'^2_o}{k_o^2 + k'^2_o} \right] \quad \text{with } \xi_0 = \frac{\left(\alpha_n - \alpha_p\right)}{\left(\alpha_n + \alpha_p\right)}$$

Before irradiation there is only one defect in the sample, the EL2 defect and we have $k'^2_0=0$. The expression reduces to the expression of the one defect electron-hole competition model [25]. When increasing irradiation dose we create two defects H3 and E4 close to mid-gap. Considering the results of absorption measurements we can consider that H3 has the greatest influence on the absorption spectra at the two wavelengths we use (i.e. 1.06μm and 1.32μm). The H3 defect will then act as a secondary defect coupled with valence band and introduced with a concentration proportional to the dose of irradiation (Fig.5). We neglect the redistribution of charges inside the main defect EL2 and then suppose that ξ_0 does not change with increasing irradiation. Then the only effect of irradiation is an increase of k'^2_0 starting from a zero value.

Here we have to consider two cases depending on the wavelength of study. At 1.06μm we have, before irradiation, $\xi_0>0$ ($\alpha_n>\alpha_p$) which means that factor $k_o^2\xi_0 - k'^2_o$ will decrease with increasing k'^2_0 due to a competition between the two terms. We observe then a decrease of the photorefractive gain down to a total cancellation of the gain. At 1.32μm the two defects have the same acceptor nature with $\xi_0<0$ ($\alpha_n<\alpha_p$) for the EL2 main defect. Term $-\left(k_o^2|\xi_0| + k'^2_o\right)$ is always negative and never changes its sign when we increase k'^2_0. The reduction factor $\frac{k_o^2\xi_0 - k'^2_o}{k_o^2 + k'^2_o}$ changes only slightly and then the irradiation has little influence on the photorefractive gain at 1.3μm as observed experimentally.

V. CONCLUSION

The effect of electron irradiation on the photorefractive properties of semi-insulating GaAs crystals has been studied. A characterization of the irradiated samples by EPR, absorption and conductivity measurements shows that the EL2 occupation ratio can be increased by irradiation up to a value of ≈1. They also reveal that the H3 hole trap, which gives rise to a level at E_V+0.71eV, is responsible for the absorption band at 1.3μm. This H3 defect modifies the PR effect in the irradiated samples. The disappearance of the PR gain at 1.06μm and the absence of variation of the gain at 1.32μm with increasing irradiation dose

are due to a competition between the EL2 defect and the H3 defect. The measurements and model presented here show that the influence of a second defect in the PR effect is only possible if this defect is very close to the Fermi level at mid-gap.

Acknowledgments : P. Delaye thanks Dr. B. Briat for his help during the low temperature absorption experiments conducted in his laboratory (ESPCI). This work was supported by Direction des Recherches Etudes et Techniques (DRET).

References :

[1] A.M. Glass, A.M. Johnson, D.H. Olson, W. Simpson, A.A. Ballman. Appl. Phys. Lett. 44, 948 (1984)

[2] A. Partovi, E.M. Garmire, G.C. Valley, M.B. Klein. Appl. Phys. Lett. 55, 2701 (1989)

[3] P. Delaye, L.A. de Montmorillon, H.J. von Bardeleben, G. Roosen. Appl. Phys. Lett. 64, 2640 (1994).

[4] Ph. Delaye, P.U. Halter, G. Roosen. Appl. Phys. Lett. 57, 360 (1990).

[5] R.S. Rana, D.D. Nolte, R. Steldt, E.M. Monberg, J. Opt Soc. Am. B 9, 1614 (1992).

[6] D. Pons, J.C. Bourgoin. J. Phys. C. 18, 3839 (1985)

[7] H.J. von Bardeleben, J.C. Bourgoin. J. Appl. Phys. 58, 1041 (1985).

[8] Y.Q. Jia, H.J. von Bardeleben, D. Stievenard, C. Delerue. Mat. Science Forum 83-87, 965 (1992).

[9] G.M. Martin, A. Mitonneau, A. Mircéa. Electron. Lett. 13, 191 (1977)

[10] A. Mitonneau, G.M. Martin, A. Mircéa. Electron. Lett. 13, 666 (1977)

[11] G.C. Valley, S.W. McCahon, M.B. Klein. J. Appl. Phys. 64, 6684 (1988)

[12] G. Guillot. Rev. Phys. Appl. 23, 833 (1988).

[13] Y.Q. Jia, H.J. von Bardeleben, D. Stievenard, C. Delerue. Proc. 21st Int. Conf. Physics of Semiconductors, p.1541 (1993) (World Scientific).

[14] R.J. Wagner, J.J. Krebs, G.H. Strauss, A.M. White. Solid State Commun. 36, 15 (1980)

[15] D.T.F. Marple. J. Appl. Phys. 35, 1241 (1964).

[16] J.S. Blakemore.J. Appl. Phys. 53, R123 (1982).

[17] F.X. Zach, A. Winnacker. Jap. J. Appl. Phys. 28, 957 (1989).

[18] P. Silverberg, P. Omling, L. Samuelson. Appl. Phys. Lett. 52, 1689 (1988)

[19] G. Vincent, D. Bois, A. Chantre. J. Appl. Phys. 53, 3643 (1982)

[20] S. Loualiche, A. Nouailhat, G. Guillot, M. Gavand, A. Laugier, J.C. Bourgoin. J. Appl. Phys. 53, 3643 (1982)

[21] A. Chantre, G. Vincent, D. Bois. Phys. Rev. B23, 5335 (1981)

[22] M. Kaminska, J.M. Parsey, J. Lagowski, H.C. Gatos. Appl. Phys. Lett. 41, 989 (1982)

[23] Ph. Delaye, H.J. von Bardeleben, G.Roosen, in Digest of Topical Meeting on Photorefractive Materials, Effects and Devices IV (6-10 August 1993, Kiev) Paper FrC02.

[24] N.V. Kukhtarev, V.B. Markov, S.G. Odulov, M.S. Soskin, V.L. Vinetskii. Ferroelectrics 22, 949-961 (1979).

[25] F.P. Strohkendl, J.M.C. Jonathan,R.W. Hellwarth. Opt. Lett. 11, 312 (1986)

[26] C.A. Berseth, C. Wuethrich, F.K. Reinhart. J. Appl. Phys. 71, 2821 (1992)

[27] J.C. Fabre, J.M.C. Jonathan, G. Roosen. Opt. Comm. 65, 257 (1988).

[28] P.Tayebati. J. Opt. Soc. Am. B9, 415 (1992)

Figure Captions

Figure 1 : EPR spectrum of the arsenic antisite (top curve) and of the gallium antisite (bottom curve).

Figure 2 : Absorption spectra at room temperature (T=300K) of non irradiated sample (D2) and of sample D8 (irradiation dose of 5x 10^{16} $e^-.cm^{-2}$).

Figure 3 : Absorption spectra at T=77K of non irradiated sample (D2), before (1) and after (2) quenching of EL2.

Figure 4 : Absorption spectra at T=77K of non irradiated sample (D2), of sample D4 (irradiation dose of $2x10^{16}e^-.cm^{-2}$) and of sample D8 (irradiation dose of $5x10^{16}e^-.cm^{-2}$) after quenching of EL2.

Figure 5 : Absorption at λ=1.32μm at T=77K after quenching of EL2 as a function of the irradiation dose.

Figure 6 : Hole photoionization cross-section spectra from defect H3 [20].

Figure 7 : Energy-band diagram of crystal with a main hole-electron trap (with a total concentration N_T) and a secondary hole trap (with a total concentration N'_T).

Table Captions

Table 1 : Traps created by room temperature electron irradiation [6] (see text for symbol definitions).

Table 2 : Concentrations of defects measured in electron irradiated samples by electron paramagnetic resonance.

Table 3 : Room temperature absorption of samples at λ=1.06μm and at λ=1.32μm as a function of the irradiation dose.

Table 4 : Dark conductivity σ_d and photoconductivity σ_{ph} at λ=1.06μm and at λ=1.32μm as a function of the irradiation dose.

Table 5 : Photorefractive gain Γ, at λ=1.06μm and at λ=1.32μm, as a function of the irradiation dose.

Trap	T_o(K)	τ (cm^{-1})	E_e (eV)	σ_a(cm^2)	β (s^{-1})
E1	20	1.5	0.045	2.2×10^{-15}	7×10^{9}
E2	60	1.5	0.14	1.2×10^{-13}	9×10^{9}
E3	160	0.4	0.30	6.2×10^{-15}	8×10^{5}
E4	310	0.08	0.76	3.1×10^{-14}	4×10^{-2}
E5	360	0.1	0.96	1.9×10^{-12}	8×10^{-4}
H0	50	0.8	0.06	1.6×10^{-16}	2×10^{9}
H1	150	0.1 - 0.7	0.29	5×10^{-15}	7×10^{6}
H2	190	-	0.41	2×10^{-16}	2×10^{4}
H3	340	≈ 0.2	0.71	1.2×10^{-14}	8×10^{-1}

Table 1

Samples	total [As_{Ga}^{+}] (cm^{-3})	quenchable[As_{Ga}^{+}] (cm^{-3})	[Ga_{As}^{-}] (cm^{-3})
D2	$6.6x10^{15}$	$6.6x10^{15}$	0
D5	$9.2x10^{15}$	$8x10^{15}$	$1.5x10^{15}$
D8	$9.1x10^{15}$	$7x10^{15}$	$5.0x10^{15}$

Table 2

Samples	Irradiation dose (x 10^{16} $e^-.cm^{-2}$)	α (1.06 μm) (cm^{-1})	α (1.32 μm) (cm^{-1})
D2	0	0.95	0.24
D5	1	1.25	0.49
D4	2	1.84	0.95
D6	3	2.30	1.22
D7	4	2.47	1.29
D8	5	2.90	1.58

Table 3

Sample	$\sigma_d(\Omega^{-1}cm^{-1})$	$\sigma_{ph}(1.06\ \mu m)$ $(\Omega^{-1}cm^{-1})$	$\sigma_{ph}(1.32\ \mu m)$ $(\Omega^{-1}cm^{-1})$
D2	3.8×10^{-9}	214×10^{-9}	470×10^{-9}
D5	5.2×10^{-9}	51×10^{-9}	200×10^{-9}
D4	7.9×10^{-9}	23.4×10^{-9}	82×10^{-9}
D6	10.4×10^{-9}	22.6×10^{-9}	63×10^{-9}
D7	29.8×10^{-9}	33.5×10^{-9}	59×10^{-9}
D8	8.2×10^{-9}	7.7×10^{-9}	13×10^{-9}

Table 4

	Γ (cm^{-1})			
Wavelength	λ = 1.06 μm		λ = 1.32 μm	
Grating spacing	0.87 μm	3 μm	1.07 μm	2.1 μm
D2	0.32	0.11	- 0.12	- 0.085
D5	0.44	0.15	- 0.14	- 0.10
D4	0.28	0.10	-0.14	- 0.09
D6	0.25	0.08	- 0.13	- 0.11
D7	0.19	0.07	- 0.12	- 0.095
D8	≈ 0	≈ 0	- 0.14	- 0.095

Table 5

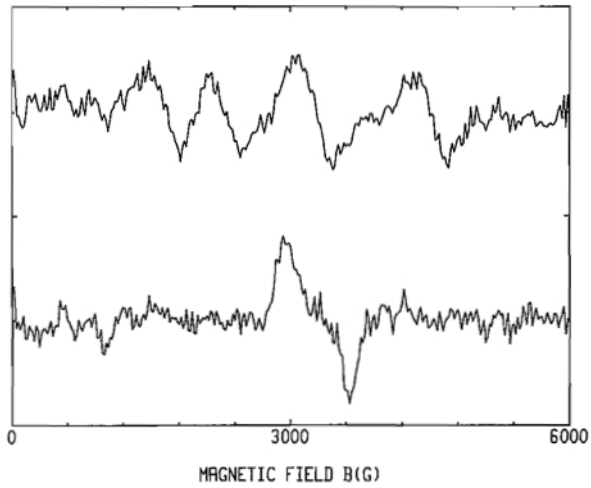

Figure 1

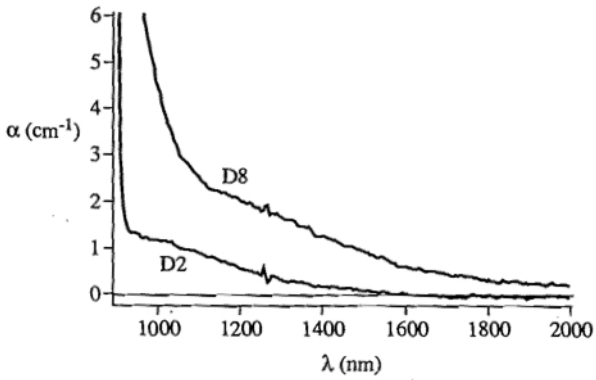

Figure 2

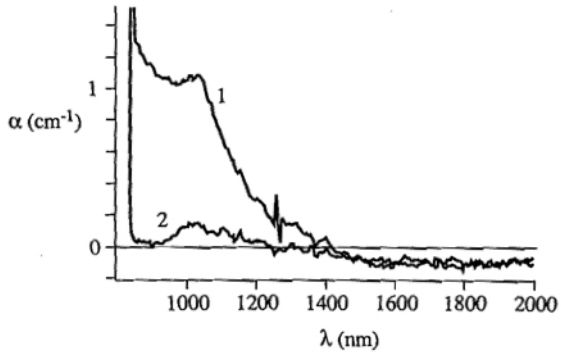

Figure 3

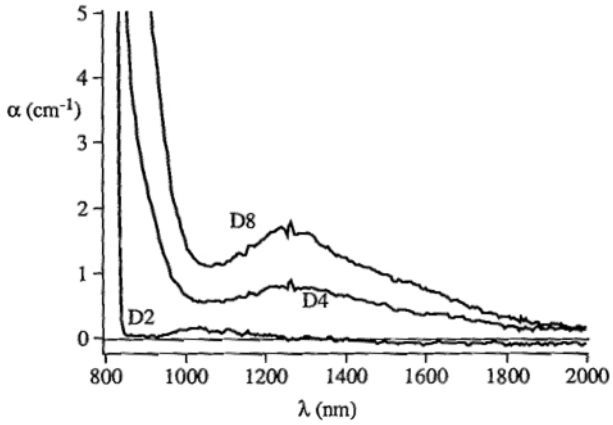

Figure 4

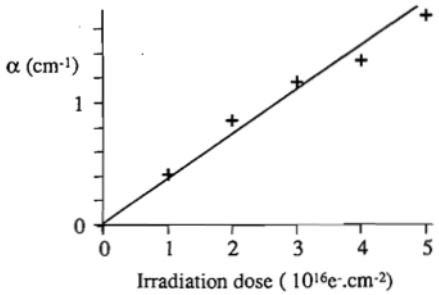

Figure 5

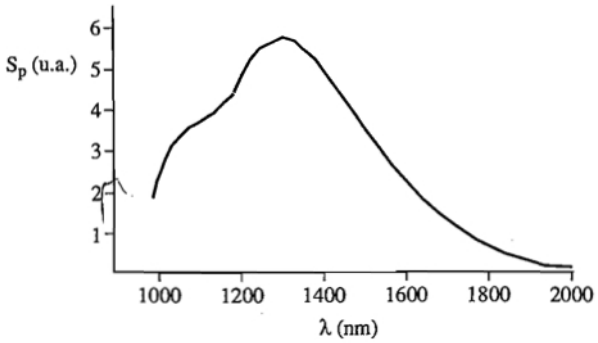

Figure 6

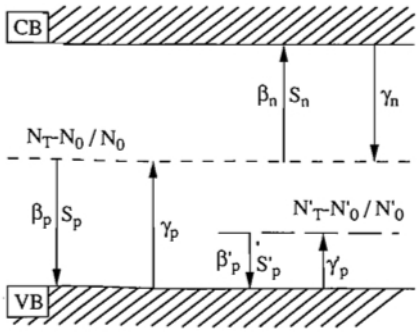

Figure 7